Journal of Ceramic Processing Research. Vol. 20, No. 2, pp. 133~138 (2019)

J O U R N A L O F
Ceramic Processing Research

Mechanical properties evaluatin of alumina-zirconia-spinel ceramic composites using ultrasonic pulse velocity

B. M. Cunha, V. T. S. Aragão, C. O. D. Martins and R. M. P. B., Oliveira
Department of Materials Science and Engineering, UFS, São Cristóvão, SE, Brazil, 49100-000

The evaluation of mechanical properties is essential to the performance guarantee of the material. However, this process is very complex for ceramic materials due to the variety of defects of such material. The aim of this work was to investigate the use of ultrasonic velocity measurements to the determination of mechanical properties in ceramic composites. To accomplish this, seven batches of alumina/zirconia, alumina/spinel and alumina/zirconia/spinel refractories were grinded, uniaxially pressed at 100 MPa and sintered at 1550 °C. The evaluation of ultrasonic pulse velocity (UPV) was performed in commercial equipment with a transducer of 5 MHz. The results showed that the addition of zirconia and spinel to the alumina matrix increased the compression resistance of the matrix in 75%. Furthermore, exponential equations relating mechanical properties and UPV were found and it was observed the existence of an intrinsic relation between these parameters.

Key words: Alumina, Composite, UPV, Spinel, Zirconia.

Introduction

Ultrasonic pulse velocity (UPV) is one of the most common nondestructive test method. It has a wide field of application, not only in finding structural defects in materials, but also in the materials characterization [1]. One of the major areas of study concerning nondestructive tests involves the correlation between this parameter and some properties of materials [2, 3, 4]. However, although there are many works on metals, the application of this type of test in ceramic materials needs to be studied more due to the variety of factors that can affect the results [3].

In ceramic materials, the properties of the sintered materials are tightly related to the processing route, sintering temperature, materials composition, structure and others [4]. Besides, this type of material presents a lack of reproducibility that requires the fabrication of lots of samples to achieve more accurate results, especially in mechanical tests [3]. Some studies have developed the area by comparing the nondestructive tests with physical properties of red ceramics and refractories [5]. Berutti *et. al.* [3] obtained an equation of quadratic nature between the density and the UPV measurements of alumina refractories. From this relation, it was possible to correlate ultrasonic wave velocity with the degree of sintering of the materials studied. Özkan and Yayla [4] have founded an intrinsic relation between the physical properties, the sintering temperature and UPV of red ceramics. It was found that the ultrasonic pulse velocity increased as the sintering temperature and, consequently, the density of red ceramics became bigger. Despite this progress, the UPV measurements are not used yet as a routine characterization technique for the mechanical properties of ceramic materials. These properties are usually measured by destructive tests which usually are laborious, cause requires the sample preparation; expensive; and, in some cases, unfeasible cause affects the structural features of the samples [6].

To aid the development of the field and to fill some gaps in the area, this work aims to study the relation between UPV measurements and the mechanical resistance of porous ceramic materials. This type of material is extensively used in acoustic and thermal insulation, as membranes, or orthopedic implants [7, 8, 9]. Besides, it has its mechanical properties intrinsically related to the type and format of the pores [10, 11, 12]. As one of the parameters that influences the ultrasonic velocity is the presence of porosity, the study of UPV in ceramic materials is of extreme importance to develop a method to control the material during the productive process or to do a quality control process [13].

Methodology

Raw materials and powder processing

The raw materials used in this work were calcined alumina (>99% Al_2O_3), monoclinic zirconia (>97% ZrO_2) and magnesium aluminate (>95% $MgAl_2O_3$).

*Corresponding author:
Tel : +55-79-3194-6344
Fax: +55-79-3194-6888
E-mail: rosaneboliveira@gmail.com

Table 1. Batch design of the investigated samples.

Group	Formulation	Alumina (wt.%)	Zirconia (wt.%)	Magnesium aluminate (wt.%)
Control group	A	100	-	-
AZ	A5Z	95	5	-
	A20Z	80	20	-
AS	A5S	95	-	5
	A20S	80	-	20
AZS	A10S10Z	80	10	10
	A20S20Z	60	20	20

Table 2. Sintering curve of the electrical furnace.

Temperature (ºC)	Velocity (ºC/min)	Dwell Time (min)
300	5	20
400	5	10
600	5	10
1000	2	10
1200	1	10
1350	1	120

Table 3. Mean particle size of the raw powders.

Raw powders	Mean particle size (μm)			Area (m^2/g)
	d(0.1)	d(0.5)	d(0.9)	
Alumina	3,136	6,748	19,206	1,2
Zirconia	2,054	7,477	18,809	1,41
Magnesium aluminate	4,672	20,650	52,882	0,672

Table 4. Chemical composition of the raw materials.

Oxides	Alumina	Zirconia	Magnesium aluminate
Al_2O_3	99,77	-	73,28
CaO	0,03	-	0,29
CuO	-	-	-
MgO	-	-	25,54
SiO_2	-	0,50	0,42
Na_2O	0,19	-	0,26
Fe_2O_3	-	-	0,12
Nb_2O_5	-	-	0,1
ZrO_2	-	97,78	-
Y_2O_3	-	-	-
TiO_2	-	0,20	-
HfO_2	-	1,52	-

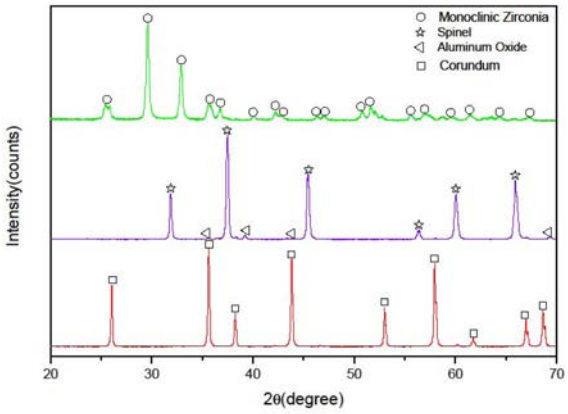

Fig. 1. XRD pattern of the raw powders. In green for monoclinic zirconia, in purple for spinel, and in red for alumina.

Alumina-zirconia composites. An organic binder of polyvinyl alcohol ([-CH_2CHOH-]n, Neon Co.) and ethylene glycol ($HOCH_2CH_2OH$ >= 99%, Sigma-Aldrich) were added to the raw powders to facilitate the conformation [14].

Seven batches were formulated by varying the weight percentage of the raw materials. In order to facilitate the results visualization, the confectioned formulations were divided into groups as described in Table 1. The raw powders were mixed with zirconia balls for 30 min in a planetary mill (RETSCH, PM 100 model) at 250 rpm and in the presence of 5 wt.% of binder. This procedure was followed by the uniaxial pressing at 100 MPa of the powders into cylindrical compacts of 10 mm diameter and approximately 13 mm height. These compacted samples were sintered in an electrical furnace at 1550 ºC for 2 hrs and under a heating rate of 1 ºC/min. The sintering curve is described at Table 2.

Characterization techniques

The particle size of used raw materials was identified by the laser diffraction technique in Malvern equipment (Mastersize 2000 model) using deionized water as dispersant. The mean particle sizes (d0.5) of alumina, zirconia and magnesium aluminate powders were 6.748, 7.477 and 20.650 μm, respectively (Table 3).

The chemical composition of the raw materials was carried out by X-ray Fluorescence (S8 Tiger, Bruker AXS). The results are described in Table 4.

The X-ray diffraction (XRD) was used to recognize the crystalline phases of the materials in a Shimadzu equipment, XRD-600 model, with Cu Kα radiation (λ = 1,5418Å) produced at 40kV and 40 mA in the 2θ range of 20° and 70°. The diffraction pattern of the raw materials is shown in Fig. 1.

Densification parameters were determined according ASTM C20-00 by Archimedes method. Five samples of each batch were dried in a muffle furnace at 120 ºC for 2 hr for the moisture removal. At room temperature, the specimens were weighed for determination of dry mass and the measurements of height and diameter were performed. After that, the bodies were heated in water bath and remained for 4 hours at 100 ºC. 24

hours later the values of immersed and satured water were measured. With those results, linear retraction, water absorption, apparent porosity and apparent density were determined by the following equations, respectively.

$$R = \left[\frac{(L_0 - L)}{L_0}\right] \times 100 \quad (1)$$

$$\mathrm{AA} = \frac{[MS_{AT} - M_{Dry}]}{M_{Dry}} \times 100 \quad (2)$$

$$\mathrm{PA} = \left[\frac{[MS_{AT} - M_{Dry}]}{MS_{AT} - MI}\right] \times 100 \quad (3)$$

$$\mathrm{DA} = \frac{M_{Dry}}{(MS_{AT} - MI)} \cdot \rho L \quad (4)$$

Uniaxial compression test was carried out in Instron equipment (3385 model) applying a crosshead speed of 0.5 mm/min. Three measurements were performed for each batch and the mean value of these values was determined as the formulation resistance.

Ultrasonic velocity measurements (UPV) were performed by using a SIUI equipment model CTS-59 and a transducer with nominal frequency of 5MHz. Methylcellulose was used as coupling agent between the sample and the transducer.

The ultrasound has the capacity of compute the waves travel time from the transducer to the interface between the sample and the surface under it. It gives as output the ultrasonic pulse velocity measured by dividing the path length by the transient time. Thus, as well as the mechanical properties, this value is extremely affected by any defect or imperfection present in the material. Therefore, this work aims to investigate the relation between those two properties in ceramic materials.

Results and Discussion

Phase analysis of sintered samples

The XRD patterns of the sintered bodies are shown in Fig. 2 to Fig. 4. In group AZ, monoclinic zirconia and alpha alumina are the major phases and tetragonal zirconia peaks are gradually increased by the addition

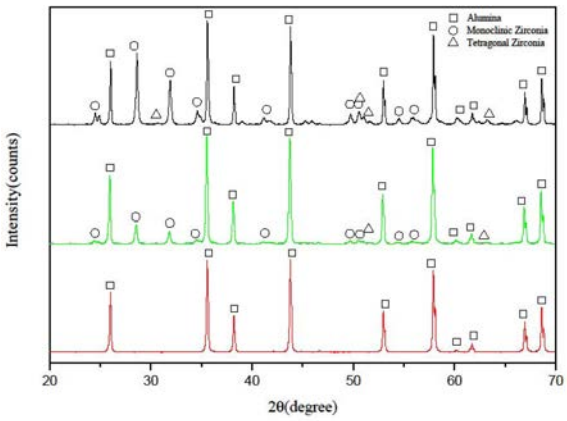

Fig. 2. XRD pattern of AZ group. Upwards are shown the diffraction pattern of A, A5Z and A20Z.

of zirconia. This increase is probably due to a volumetric expansion of zirconia particles during sintering which acts as a tetragonal phase stabilizer [15]. This phenomenon can improve the mechanical properties of the bodies, because when a load is applied, the particles expand and act as a barrier against the crack propagation [16-18].

In the AS group, the spinel peaks were more intense with the addition of 20 wt.% of spinel.

In the last group, alpha alumina, tetragonal and monoclinic zirconia and spinel were detected. However, the quantity of tetragonal zirconia peaks in the formulation A20S20Z did not change. Thus, the magnesium aluminate was not effective in stabilize the zirconia.

Physical Properties

Physical properties of the batches are depicted in Table 5. During sintering, various physicochemical processes occur which causes the increase in density and decrease in porosity by the rearrangement of the particles [19]. The composition A5S presents the highest values for water absorption and apparent porosity among the other groups. Besides, this batch showed a liner retraction lower than alumina composites. In this case, there was a considerable formation of pores, justified by the bad accommodation of the particles and the

Table 5. Physical properties of the sintered composites.

Group	Formulations	Density (g/cm^3)	Apparent porosity (%)	Linear Retraction (%)	Water absorption (%)
	A	2.69 ± 0.03	30.09 ± 1.54	4.55 ± 0.45	11.19 ± 0.64
AZ	A5Z	2.77 ± 0.02	29.06 ± 0.83	5.41 ± 0.75	10.5 ± 0.36
	A20Z	3.05 ± 0.03	25.94 ± 1.39	6.42 ± 0.41	8.50 ± 0.54
AS	A5S	2.61 ± 0.02	32.39 ± 1.20	3.67 ± 0.45	12.42 ± 0.55
	A20S	2.8 ± 0.04	27.13 ± 0.93	5.48 ± 0.46	9.71 ± 0.38
AZS	A10S10Z	2.86 ± 0.03	27.46 ± 0.82	5 ± 0.52	9.61 ± 0.36
	A20S20Z	3.14 ± 0.12	24.12 ± 0.58	5.68 ± 0.33	7.70 ± 0.31

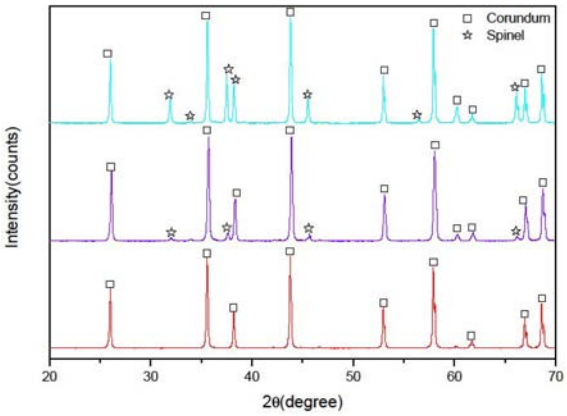

Fig. 3. XRD pattern of AS group. Upwards are shown the diffraction pattern of A, A5S and A20S.

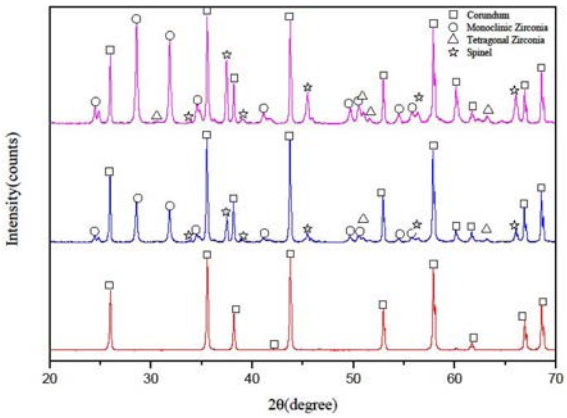

Fig. 4. XRD pattern of AZS group. Upwards are shown the diffraction pattern of A, A10S10Z and A20S20Z.

consequent increase in porosity and decrease in density [20].

In the other batches, the addition of second phases caused an improvement on the properties. Alumina-zirconia composites obtained the largest values of linear retraction. This fact shows that a better placement of particles was obtained after sintering. Density of samples with zirconia increased as the content of second phase increased. This fact is due to the high density of this raw material and the volume expansion of zirconiauf particles.

In the group AZS, the density of the batch A20S20Z was 16% higher than alumina. This value is very close to the increase of 13% in the formulation A20Z. However the presence of magnesium aluminate powder developed the properties of these composites. Besides that, it can be noted that the apparent porosity and water absorption decreases from formulation A20Z to A20S20Z.

Mechanical properties

In Fig. 5, the measured values for compressive

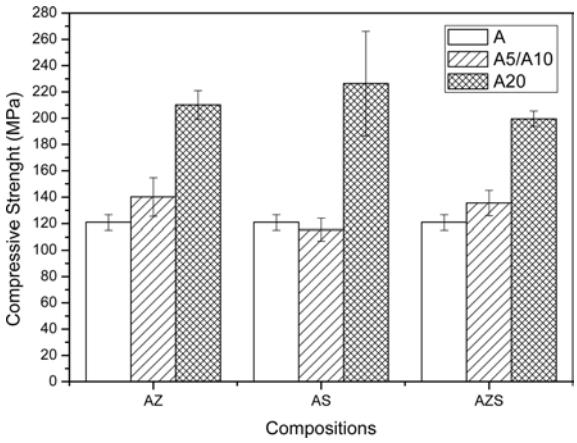

Fig. 5. Uniaxial compression results separated per groups. (Legend: A = Alumina batch; A5/A10 = Formulations A5Z, A5S and A10S10Z, respectively; A20 = Formulations A20Z, A20S and A20S20Z, respectively).

strength are shown. The raise in zirconia content in groups AZ and AZS lead to an increase of more than 60% in the mechanical properties of the formulations. This result was expected due to the enhancing of density and decline in porosity as the content of zirconia increased as well as the good compaction of the matrix particles [19]. Moreover, this is also attributed to the tetragonal to monoclinic phase transformation of zirconia particles. The compression test applies an external stress to the composite, which causes a transformation in zirconia structure from metastable phase to the stable monoclinic phase. This alteration causes a volume expansion in the zirconia particles and a consequent resistance to the crack propagation.

The A5S formulation obtained a compressive strength value lower than the control group since it has a low density and high porosity. On the other hand, the addition of 20 wt.% of magnesium spinel leads to an increase in the mechanical properties of the composite.

The compression resistance of the group AZS was improved by the addition of zirconia and spinel. Besides the toughening effect from the martensitic transformation of zirconia, this behavior is also related to the generation of residual stresses during cooling from sintering temperature due to a difference in thermal expansion coefficients of the raw materials. Therefore, during the compression load, these stresses facilitate the intergranular crack propagation and aid the improvement of the composites resistance [21].

Ultrasonic pulse velocity

The ultrasonic pulse velocity measurements agreed with the values founded in previous works [3]. In the group AZ, the decrease in velocity is related to lowering of elastic modulus with increasing zirconia [15, 22]. This behavior for the composites alumina-

Table 6. Correlation analysis between mechanical properties and UPV. (Abbreviations: UC = Uniaxial compression, V = Ultrasonic velocity).

Mechanical Test	Groups	Regression Equation	R^2
Uniaxial Compression	AZ	UC = exp(-37.172 + 0.016V – 1.413E-6V^2)	0.9475
	AS	UC = exp(240.969 – 0.0749V + 5.927E-6V^2)	0.92644
	AZS	UC = exp(66.753 – 0.0196V + 1.551E-6V^2)	0.92907

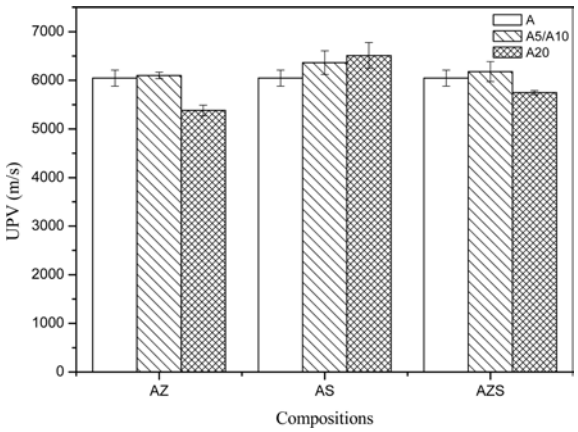

Fig. 6. UPV measurements of the batches. (Legend: A = Alumina batch; A5/A10 = Formulations A5Z, A5S and A10S10Z, respectively; A20 = Formulations A20Z, A20S and A20S20Z, respectively).

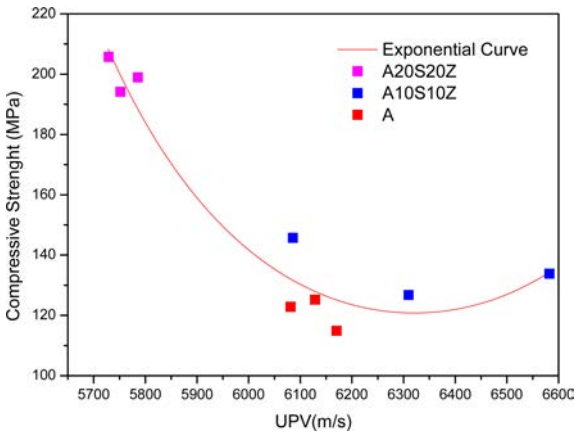

Fig. 7. Relation between UPV and compressive strength of group A10S10Z.

zirconia is a well-known fact and it is one of the main reasons for the decrease in UPV in group AZ and AZS. On the other hand, alumina-spinel composites had an increase in ultrasonic velocity due to the raise in the elasticity modulus (Fig. 6).

Correlation between UPV measurements and mechanical test

From the data obtained in the mechanical tests and in the UPV measurements, regressions equations were determined to correlate these factors using the composition as a parameter. The coefficient of determination of the equations (R^2) gives the level of variance from the plotted data and the correspondent point in the graph. Therefore, this constant must be high to affirm that the correlation is reliable. As can be detected from Table 6, all of the equations have R^2 superior to 0.9 and can be settled as reliable.

The plotted points and the respective regression equation can be seen in Fig. 7 to Fig. 9. In the graph for the compressive strength points, the higher data corresponds to the composition A20S20Z and the lower, to the A10S10Z. Likewise, for the AZ composition, formulation A20Z are the most resistant. In both plots the most resistant points have the higher velocities.

From those results, it can be observed that UPV significantly changes with the composition of the material. Besides that, other factors affect the results. The sintering temperature, for example, decreases the porosity of the composites and therefore favors the

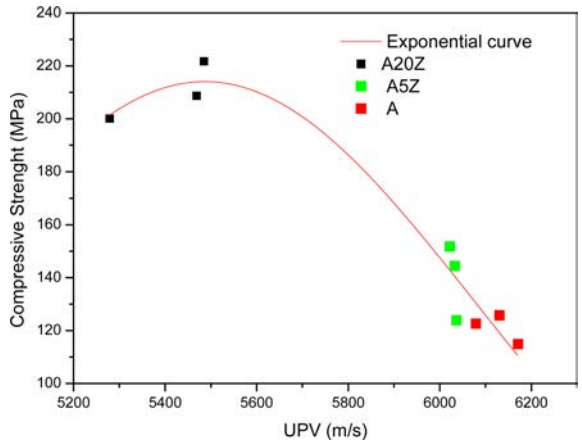

Fig. 8. Relation between UPV and compressive strength of group AZ.

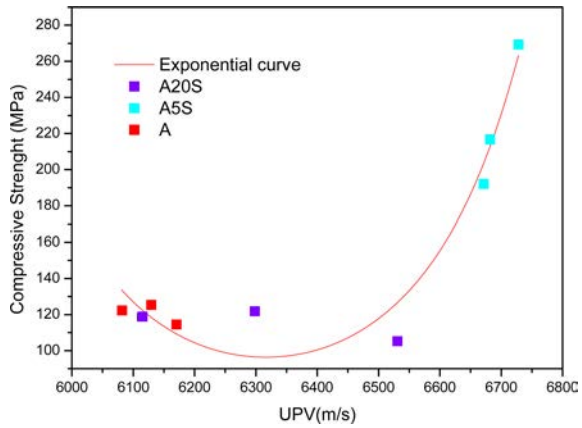

Fig. 9. Relation between UPV and compressive strength of group AS.

movement of the ultrasound.

Based on these results, it is possible to affirm that UPV measurements can be used to determine the resistance of composites alumina-zirconia-spinel. Therefore, this work provides an alternative way for the inspection and quality control process of ceramic composites. However, future works should be done with varied compositions and sintering temperatures to increase the knowledge in this area.

Conclusions

Obtaining an equation that correlates the mechanical properties with the UPV measurements of refractories is of extreme importance for a faster determination of the materials resistance. In this work, it was founded an inherent relation between compression resistance and UPV. From the results, it can be affirmed that the UPV can be used to make predictions about the progress of the mechanical properties of this type of material with varied composition.

Although the results are encouraging, there are other determinant factors influencing the founded relations and its reliability. The sintering temperature, the microstructure and other compositions are some examples. Thus, it is recommended that future works should be done to fill those gaps in literature.

Acknowledgments

The authors are grateful to the Brazilian funding agency CNPq and Capes for financial support.

References

1. M. Agrawal, A. Prasad, J.R. Bellare, A.A. Seshia, Ultrasonics 64 (2016) 186-195.
2. T. Matusinovic, S. Kurajica, J. Sipusic, Cem. Concr. Res. 34 (2004) 1451-1457.
3. F.A. Berutti, A.K. Alves, C.P. Bergmann, Mater. Des. (2010) 3996-4000.
4. İ. Özkan, Z. Yayla, Ultrasonics 66 (2016) 4-10.
5. L.-S. Chang, T.-H. Chuang, W.J. Wei, Mater. Charact. 45 (2000) 221-226.
6. H.Y. Qasrawi, Cem. Concr. Res. 30 (2000) 739-746.
7. J. Liu, Y. Li, Y. Li, S. Sang, S. Li, Ceram. Int. 42 (2016) 8221-8228.
8. X. Li, M. Gao, Y. Jiang, Ceram. Int. 42 (2016) 12531-12535.
9. X. Dong, M. Wang, A. Guo, Y. Zhang, S. Ren, G. Sui, H. Du, J. Alloys Compd. (2017) 1045-1053.
10. A.A. Al-Attar, M.A. Zaeem, S.A. Ajeel, N.E.A. Latiff, J. Eur. Ceram. Soc. 37 (2017) 1635-1642.
11. M. Han, X. Yin, L. Cheng, S. Ren, Z. Li, Mater. Des. (2017) 384-390.
12. T.T. Dele-Afolabi, M.A.A. Hanim, M. Norkhairunnisa, M. Sobri, R. Calin, Ceram. Int. 43 (2017) 8743-8754.
13. D. Pandey, S. Pandey, in "Acoustic Waves" (Sciyo, 2010) p. 397-430.
14. S.M. Ani, A. Muchtar, N. Muhamad, and J. Ghani, Ceram. Int. 40 (2014) 273-280.
15. H. Carreon, A. Ruiz, A. Medina, G. Barrera, J. Zarate, Mater. Charact. 60 (2009) 875-881.
16. C. Exare, J.-M. Kiat, N. Guiblin, F. Porcher, V. Petricek, J. Eur. Ceram. Soc. 35 (2015) 1273-1283.
17. A. Rittidech, N. Suekwamsue, Ceram. Int. 41 (2015) S123-S126.
18. M.M.S. Wahsh, R.M. Khattab, M. Awaad, Mater. Des. 41 (2012) 31-36.
19. G.I.V. Carbajal, J.L.R. Galicia, J.C. Rendo, J.L. Cuevas, C.A.G. Chavarría, Ceram. Int. 38 (2012) 1617-1625.
20. D. Casellas, M.M. Nagl, L. Llanes, M. Anglada, J. Mater. Process. Technol. 143-144 (2003) 148-152.
21. M. Khoshkalam, M.A. Faghihi-Sani, Mater. Sci. Eng., A 587 (2013) 336-343.
22. H.L.C. Pulgarin, M.P. Albano, Mater. Sci. Eng., A 639 (2015) 136-144.